# Heavy flavor production with the ATLAS experiment at LHC

Vincenzo Canale

Università di Napoli “Federico II” and INFN

LHCP2016: LUND 12/6-18/6

# Outline

A. Introduction:
   1) General framework
   2) Experimental aspects

B. Quarkonium states:
   1) $J/\psi$ and $\psi(2s)$ differential production at $\sqrt{s}$ =7-8 TeV
   2) $J/\psi$ differential non prompt production at $\sqrt{s}$ =13 TeV

C. Heavy flavour open states
   1) $f_s/f_d$ determination at $\sqrt{s}$ =7 TeV
   2) $B^{\pm}$ mass reconstruction in $B^{\pm} \rightarrow J/\psi\ K^{\pm}$ at $\sqrt{s}$ =13 TeV
   3) $D^{*\pm}$ , $D^{\pm}$ and $D_s^{\pm}$ production at $\sqrt{s}$ =7 TeV

D. Conclusions

# A.1 General framework

→ Heavy Flavor (HF) production is a crucial phenomenon to test QCD.

Charmonium production: (a) directly (*prompt*) by short lived QCD sources, (b) from decays of long-lived b-hadrons (*non-prompt*)

Non-Prompt production successfully described by :
Fixed Order Next Leading Log (FONLL)

# A.1 General framework

→ Heavy quark (HQ) production is a crucial phenomenon to test QCD.

Charmonium production: (a) directly (*prompt*) by short lived QCD sources, (b) from decays of long-lived b-hadrons (*non-prompt*)

Non-Prompt production successfully described by :
Fixed Order Next Leading Log (FONLL)

Prompt quarkonium production is unique test ground:
production "hard" scale + evolution via non-perturbative

Non Relativistic QCD prescription:
CO calculation + Long Distance Matrix Elements (from data)
→ improved agreement with data, but need coherent approach

→ major interest in ψ(2S) less affected by feed-down with respect to other states

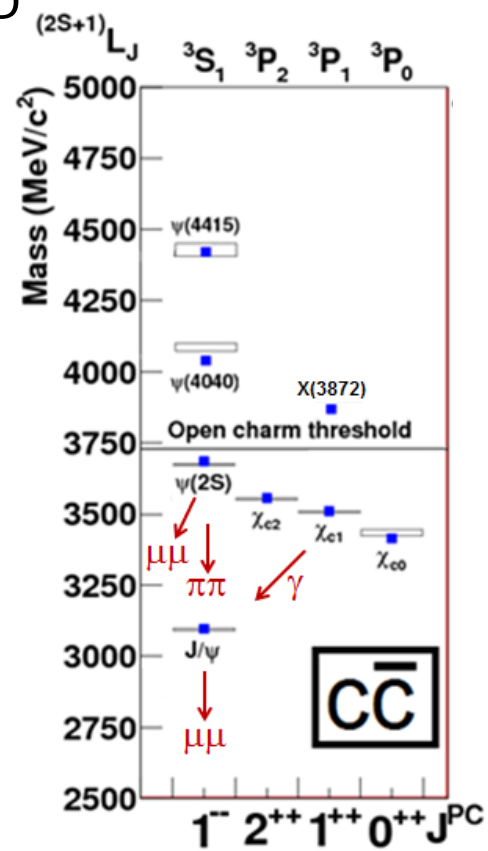

# A.1 General framework

→ Heavy quark (HQ) production is a crucial phenomenon to test QCD.

Charmonium production: (a) directly (*prompt*) by short lived QCD sources, (b) from decays of long-lived b-hadrons (*non-prompt*)

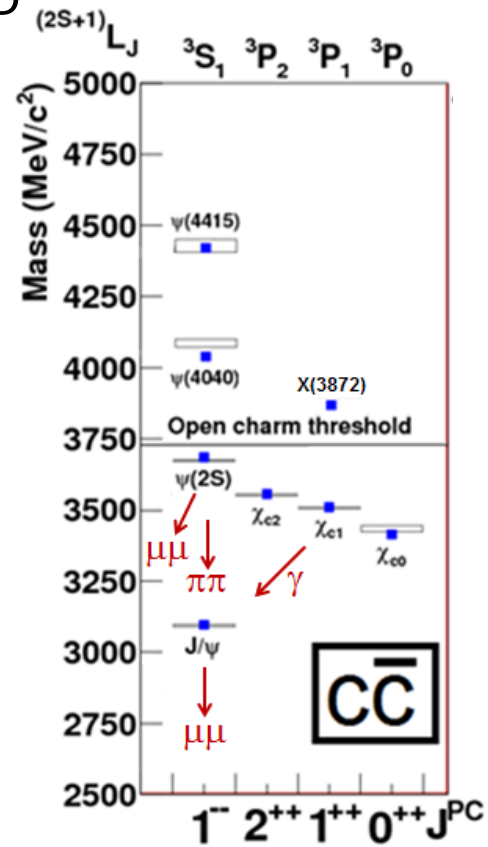


Non-Prompt production successfully described by :
Fixed Order Next Leading Log (FONLL)

Prompt quarkonium production is unique test ground:
production "hard" scale + evolution via non-perturbative

Non Relativistic QCD prescription:
CO calculation + Long Distance Matrix Elements (from data)
→ improved agreement with data, but need coherent approach

→ major interest in ψ(2S) less affected by feed-down with respect to other states

Open HF production described by FONLL:
1) satisfactory for b
2) for c →difficulty in matching different regimes ( $p_T >> m_Q$ , $p_T \sim m_Q$, $p_T << m_Q$ )

→ HF@LHC data are very important in itself (new high $p_T$ kinematic regions)
→ to understand significant background for EW, Higgs, NP sectors

# A.2 Experimental aspects

## A.2.1 Data samples

LHC machine:

- run-I:

5,1 $fb^{-1}$ at 7 TeV + 21.3 $fb^{-1}$ at 8 Tev

- run –II: 3.9 $fb^{-1}$ at 13 TeV (2015)

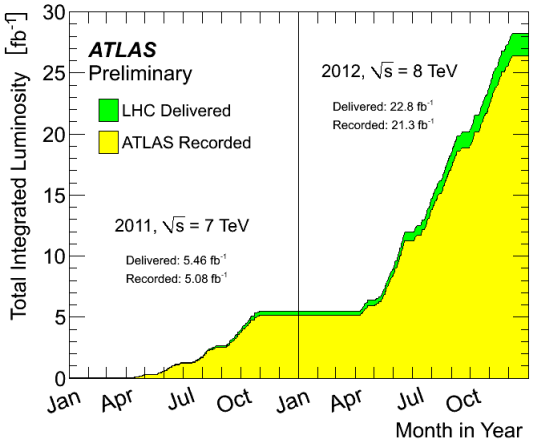


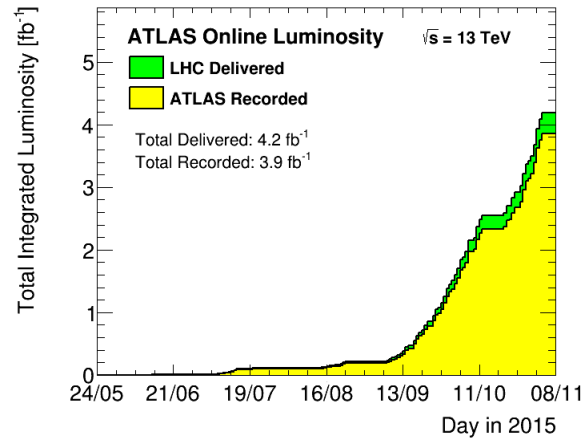

# A.2 Experimental aspects

## A.2.1 Data samples

LHC machine:

- run-I:

5,1 $fb^{-1}$ at 7 TeV + 21.3 $fb^{-1}$ at 8 Tev

- run –II: 3.9 $fb^{-1}$ at 13 TeV (2015)

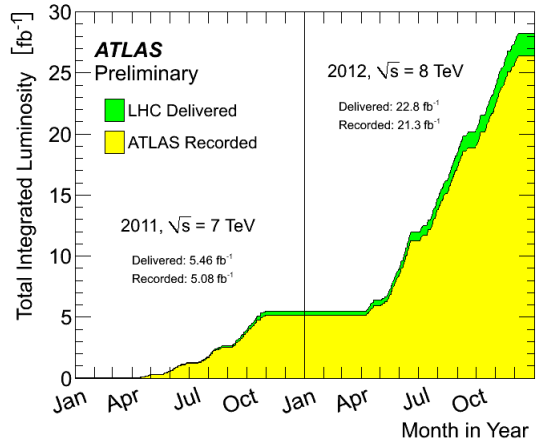


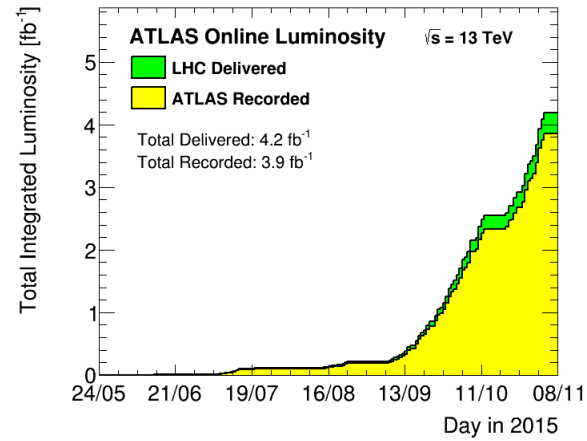


## A.2.2 Detector and trigger

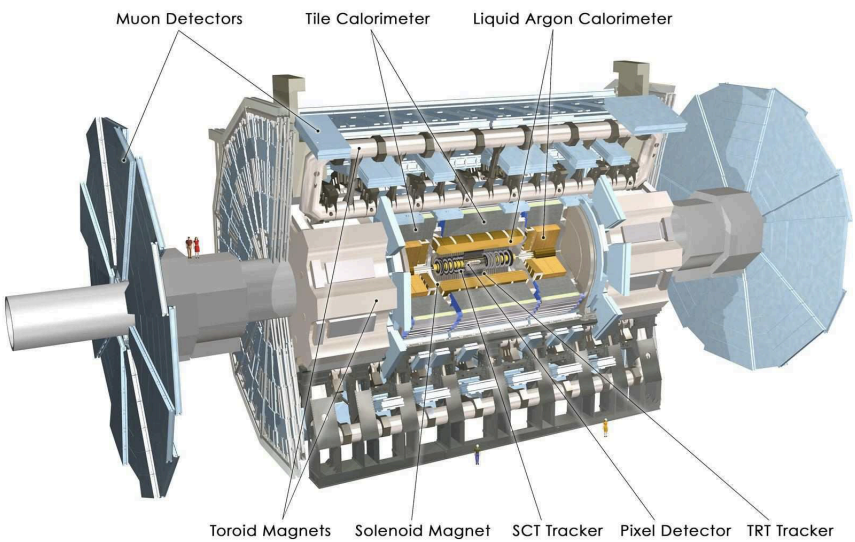


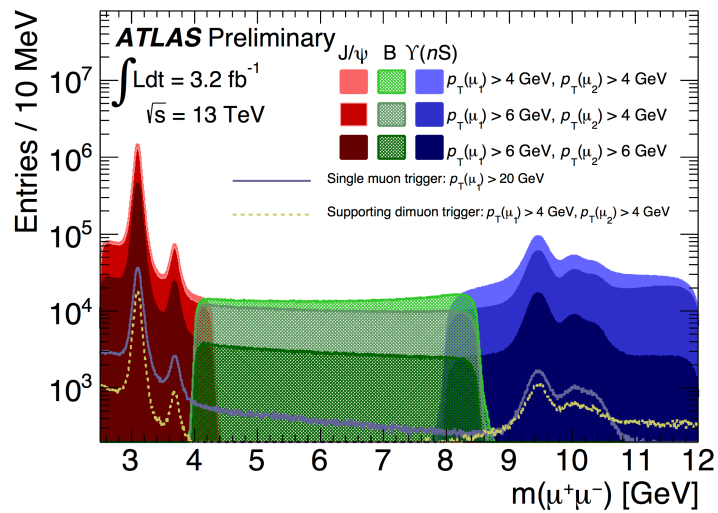


ID: $|\eta|<2.5$, $B_{sol}$ =2T, Pixels+Si+TRT

→ $\sigma_{Pt}/p_t \approx 0{,}0004\ p_t\,(\mathrm{GeV}) + 0{,}015$

MS: $|\eta|<2.7$, $\langle B_{tor}\rangle=0{,}5$ T

→ $\sigma_{Pt}/p_t \leq 0.1$ up to 1 TeV

Muon Trigger for HF physics:

- L1: di-muon $p_T^{\mu}$ thresholds: 4-6 GeV
- L2/EF: validation + vertexing + $m_{\mu\mu}$ windows

# A.2.3 Tracking, vertexing, mass and "proper" time fits

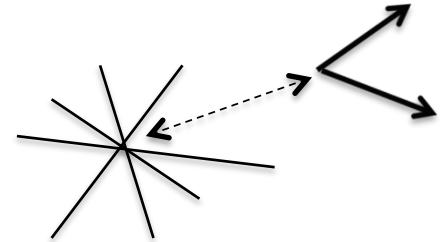

$$\text{muon pairs for "}\psi\text{"} \begin{cases} P_t \geq 4\text{GeV}, \ |\eta| < 2.3 \\ \text{opposite charge} \\ MS \xrightarrow{\text{match}} ID \text{ track} \\ \text{common vertex } \chi^2 < 20 \\ 2.6 \text{ GeV} \leq m_{\mu\mu} \leq 4.0 \text{ GeV} \end{cases}$$

pseudo proper time

$$\tau = \underbrace{\vec{L} \cdot \frac{\vec{P}_T^{(\mu\mu)}}{P_T^{(\mu\mu)}}}_{L_{xy}} \times \frac{m_{\mu\mu}}{P_T^{(\mu\mu)}}$$

# A.2.3 Tracking, vertexing, mass and "proper" time fits

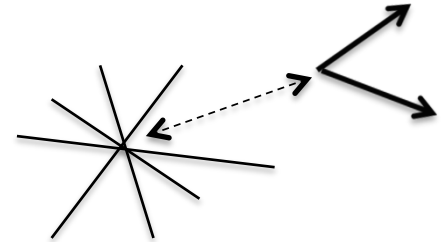

muon pairs for "$\psi$"

$$\begin{cases} P_t \geq 4\text{GeV}, \ |\eta| < 2.3 \\ \text{opposite charge} \\ MS \xrightarrow{\text{match}} ID \text{ track} \\ \text{common vertex } \chi^2 < 20 \\ 2.6 \text{ GeV} \leq m_{\mu\mu} \leq 4.0 \text{ GeV} \end{cases}$$

pseudo proper time

$$\tau = \underbrace{\vec{L} \cdot \frac{\vec{P}_T^{(\mu\mu)}}{P_T^{(\mu\mu)}}}_{L_{xy}} \times \frac{m_{\mu\mu}}{P_T^{(\mu\mu)}}$$

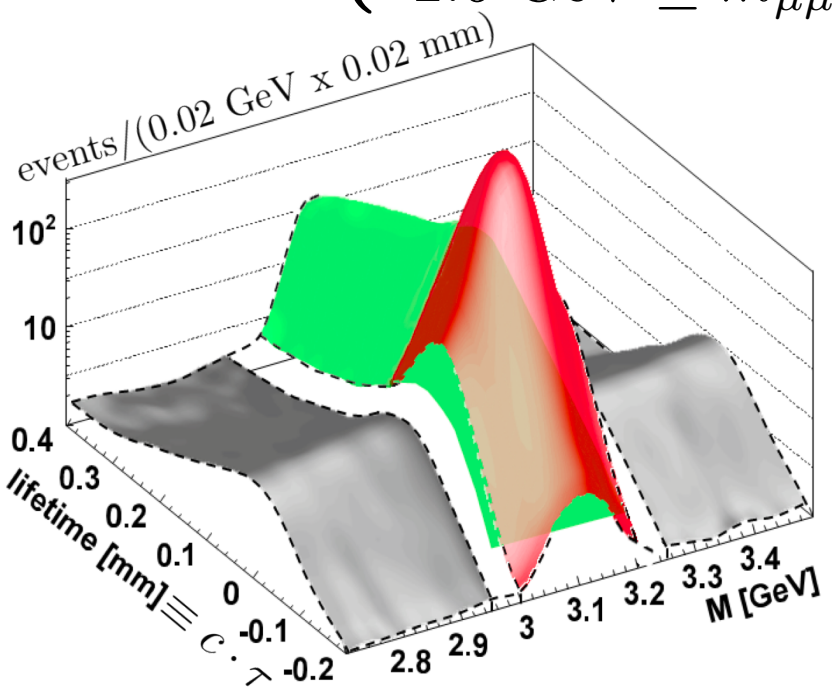


$$\Rightarrow \begin{cases} \text{P} & : \text{prompt component} \\ \text{NP} & : \text{non-prompt from B-decays} \end{cases}$$

unbinned maximum likelihood fit in 2D

$$PDF(m,\tau) = \sum_i \kappa_i f_i(m) \cdot h_i(\tau) \otimes \mathcal{R}(\tau)$$

| $i$ | Type | Source | $f_i(m)$ | $h_i(\tau)$ |
|---|---|---|---|---|
| 1 | $J/\psi$ | P | $\omega B_1(m) + (1-\omega)G_1(m)$ | $\delta(\tau)$ |
| 2 | $J/\psi$ | NP | $\omega B_1(m) + (1-\omega)G_1(m)$ | $E_1(\tau)$ |
| 3 | $\psi(2S)$ | P | $\omega B_2(m) + (1-\omega)G_2(m)$ | $\delta(\tau)$ |
| 4 | $\psi(2S)$ | NP | $\omega B_2(m) + (1-\omega)G_2(m)$ | $E_2(\tau)$ |
| 5 | Bkg | P | $F$ | $\delta(\tau)$ |
| 6 | Bkg | NP | $C_1(m)$ | $E_3(\tau)$ |
| 7 | Bkg | NP | $E_4(m)$ | $E_5(\lvert\tau\rvert)$ |

mass $\rightarrow G_i$ : Gaussian, $B_i$ : Crystal Ball
time $\rightarrow E_i$ : exponential, $\mathcal{R}$ : double Gaussian
bkg $\rightarrow C_i$ : Chebyshev, $F$ : uniform

# A.2.4 Cross section extraction

$$\frac{d^2\sigma(pp \to Q + X)}{dp_T dy} \cdot Br(Q \to \mu\mu) = \frac{N_{corr}^{Q\to\mu\mu}}{\mathcal{L} \cdot \Delta p_T \cdot \Delta y}$$

$$\begin{cases} N_{corr}^{Q\to\mu\mu} : \text{signal yield corrected for efficiency and acceptance} \\ \mathcal{L} : \text{integrated luminosity corresponding to the sample} \\ \Delta p_T(y) : \text{interval bin of the differential variable} \end{cases}$$

$$\text{8 rapidity bins}: \ 0 \leq |y^{(\mu\mu)}| \leq 2$$
$$\sqrt{s} = 7\,TeV : 8 \leq p_T^{(J/\psi)} \leq 100\text{GeV}$$
$$\sqrt{s} = 7\,TeV : 8 \leq p_T^{(\psi_{2s})} \leq \ 60\text{GeV}$$
$$\sqrt{s} = 8\,TeV : 8 \leq p_T^{(\mu\mu)} \leq 110\text{GeV}$$
$$\sqrt{s} = 13\,TeV : 8 \leq p_T^{(J/\psi)} \leq 40\text{GeV}$$

# A.2.4 Cross section extraction

$$\frac{d^2\sigma(pp \to Q + X)}{dp_T dy} \cdot Br(Q \to \mu\mu) = \frac{N_{corr}^{Q\to\mu\mu}}{\mathcal{L} \cdot \Delta p_T \cdot \Delta y}$$

$$\begin{cases} N_{corr}^{Q\to\mu\mu} : \text{signal yield corrected for efficiency and acceptance} \\ \mathcal{L} : \text{integrated luminosity corresponding to the sample} \\ \Delta p_T(y) : \text{interval bin of the differential variable} \end{cases}$$

$$\text{8 rapidity bins}: \ 0 \leq |y^{(\mu\mu)}| \leq 2$$
$$\sqrt{s} = 7\,TeV : 8 \leq p_T^{(J/\psi)} \leq 100\text{GeV}$$
$$\sqrt{s} = 7\,TeV : 8 \leq p_T^{(\psi_{2s})} \leq 60\text{GeV}$$
$$\sqrt{s} = 8\,TeV : 8 \leq p_T^{(\mu\mu)} \leq 110\text{GeV}$$
$$\sqrt{s} = 13\,TeV : 8 \leq p_T^{(J/\psi)} \leq 40\text{GeV}$$

$\varepsilon(p_T^{(\mu)}, \eta^{(\mu)})$→ efficiencies (trigger, reconstruction,…) are estimated mainly with data driven methods to reduce uncertainties (tag and probe methods, etc…)

weight for each candidate :

$$w_i^{-1} = \epsilon_i^{(reco.)} \cdot \epsilon_i^{(trig.)} \cdot \mathcal{A}_i$$

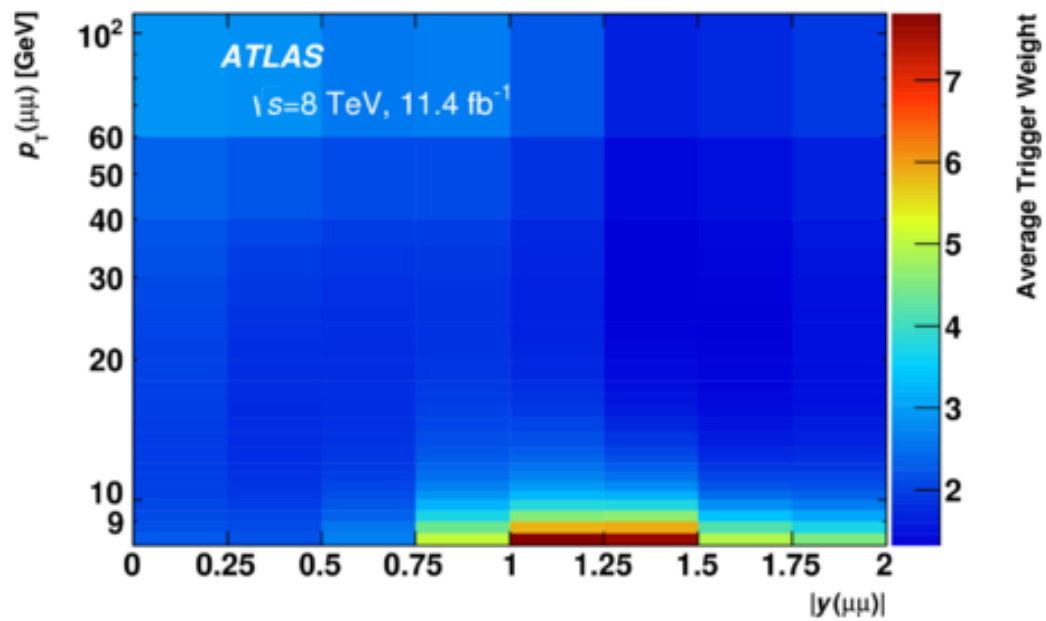

$\mathcal{A}(p_T^{(\mu\mu)}, y^{(\mu\mu)})$: the probability for a candidate that both muons pass the fiducial selection ($p_T^{(\mu)}$>4 GeV, $|\eta^{(\mu)}|$<2.3) is estimated with simulation (generator + detector)

$$\frac{d^2N}{d\cos\theta^* d\phi^*} \propto 1 + \lambda_\theta \cos^2\theta^* + \lambda_\phi \sin^2\theta^* \cos 2\phi^* + \\ + \lambda_{\theta\phi} \sin 2\theta^* \cos\phi^*$$

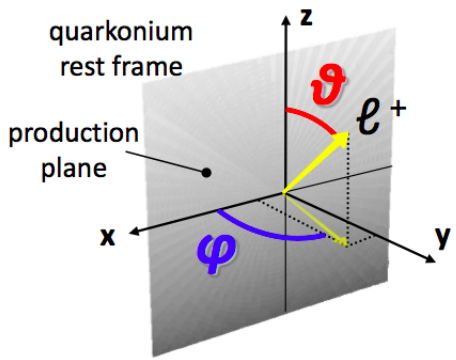


| | Angular coefficients | | |
|---|---|---|---|
| | $\lambda_\theta$ | $\lambda_\phi$ | $\lambda_{\theta\phi}$ |
| Isotropic *(central value)* | 0 | 0 | 0 |
| Longitudinal | −1 | 0 | 0 |
| Transverse positive | +1 | +1 | 0 |
| Transverse zero | +1 | 0 | 0 |
| Transverse negative | +1 | −1 | 0 |
| Off-($\lambda_\theta$–$\lambda_\phi$)-plane positive | 0 | 0 | +0.5 |
| Off-($\lambda_\theta$–$\lambda_\phi$)-plane negative | 0 | 0 | −0.5 |

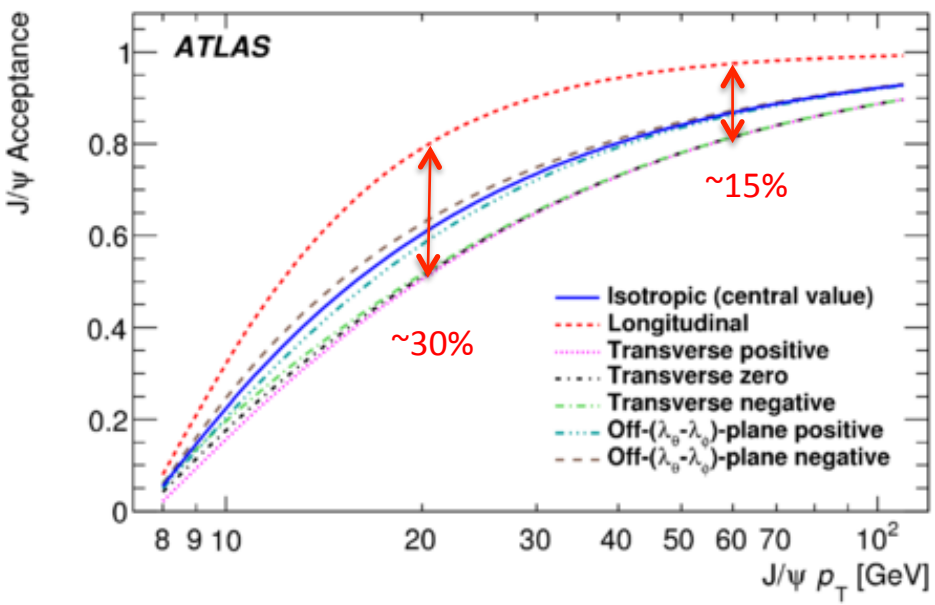


Acceptance corrections depend on the spin alignment at production:

→ use the isotropic case and consider the envelope of maximum variations in case of different polarization states;

→ dependence is reduced at high $p_T$;

→ better to explore high $p_T$ region (both theory and experiment)

# B.1 J/ψ and ψ(2s) differential production at √s =7-8 TeV

Eur.Phys.J. C76 (2016) 5, 283

$$\begin{cases} J/\psi \to \mu^+\mu^- \\ \psi(2S) \to \mu^+\mu^- \end{cases} \quad \begin{cases} 2.1\, fb^{-1} \text{ at } \sqrt{s} = 7\,\text{TeV} \\ 11.4\, fb^{-1} \text{ at } \sqrt{s} = 8\,\text{TeV} \end{cases}$$

## Examples of fit projections

√s=7 TeV
10.5<$p_t$<11.5 Gev
1.25<|y|<1.50

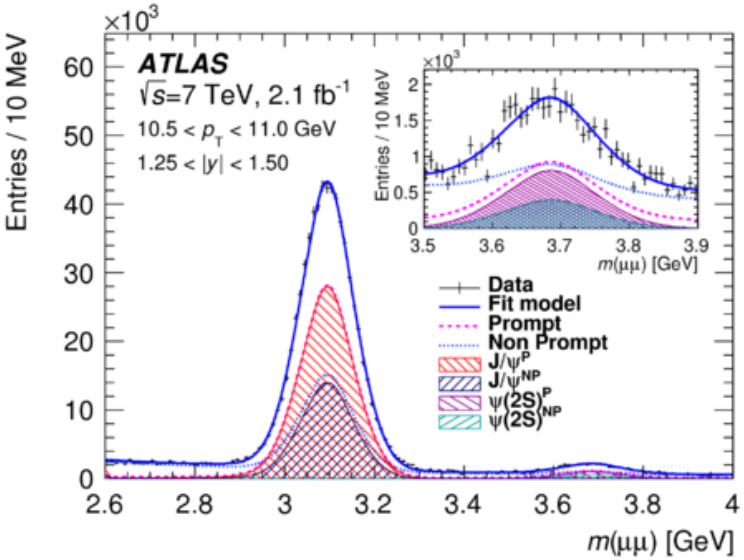


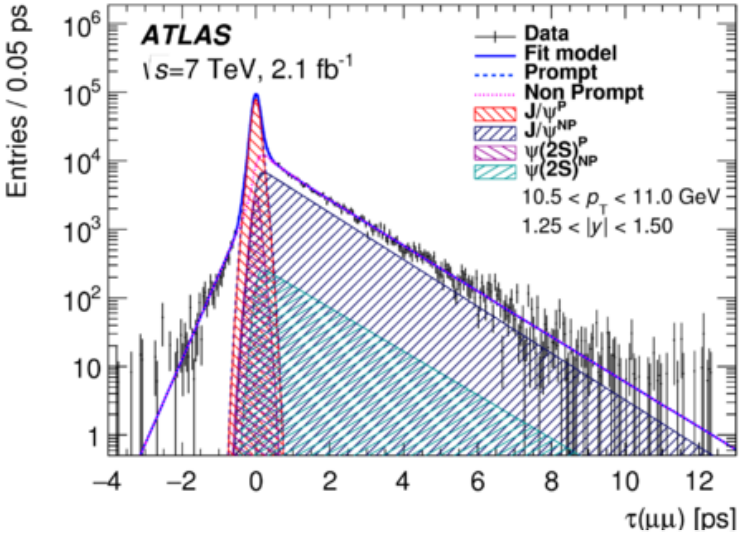


√s=8 TeV
60.0<$p_t$<110.0 Gev
|y|<0.25

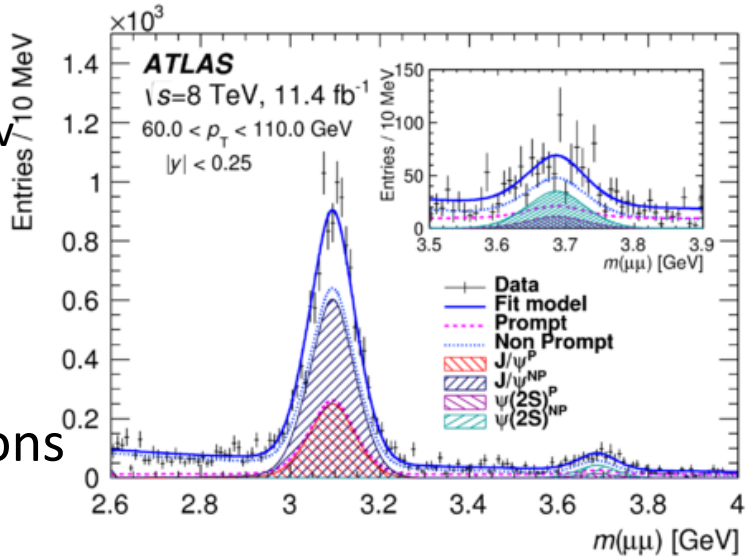


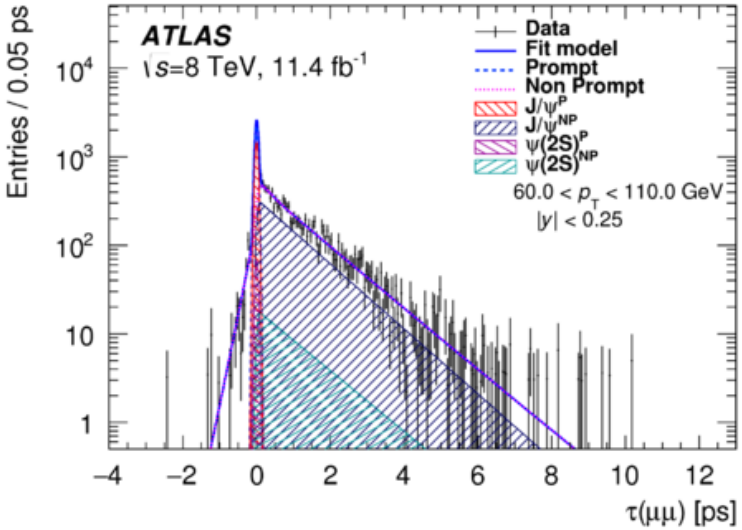


from fit yields
→ cross sections

Systematic uncertainties dominated :

- Muon trigger efficiency evaluation;
- Fit model parametrization

$$\Rightarrow \left(\frac{\Delta\sigma}{\sigma}\right)_{sys.} \sim (6 \div 8)\%$$

| | 7 TeV [%] | | | 8 TeV [%] | | |
|---|---|---|---|---|---|---|
| Source of systematic uncertainty | Min | Median | Max | Min | Median | Max |
| Luminosity | 1.8 | 1.8 | 1.8 | 2.8 | 2.8 | 2.8 |
| Muon reconstruction efficiency | 0.7 | 1.2 | 4.7 | 0.3 | 0.7 | 6.0 |
| Muon trigger efficiency | 3.2 | 4.7 | 35.9 | 2.9 | 7.0 | 23.4 |
| Inner detector tracking efficiency | 1.0 | 1.0 | 1.0 | 1.0 | 1.0 | 1.0 |
| Fit model parameterizations | 0.5 | 2.2 | 22.6 | 0.26 | 1.07 | 24.9 |
| Bin migrations | 0.01 | 0.1 | 1.4 | 0.01 | 0.3 | 1.5 |
| Total | 4.2 | 6.5 | 36.3 | 4.4 | 8.1 | 27.9 |

Prompt J/ψ: 0.75<|y|<1.00

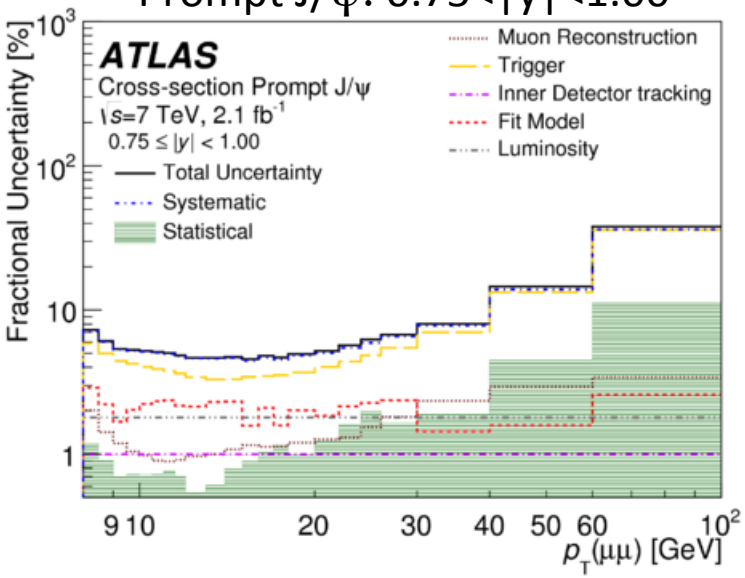


Non Prompt ψ(2S): 0.75<|y|<1.00

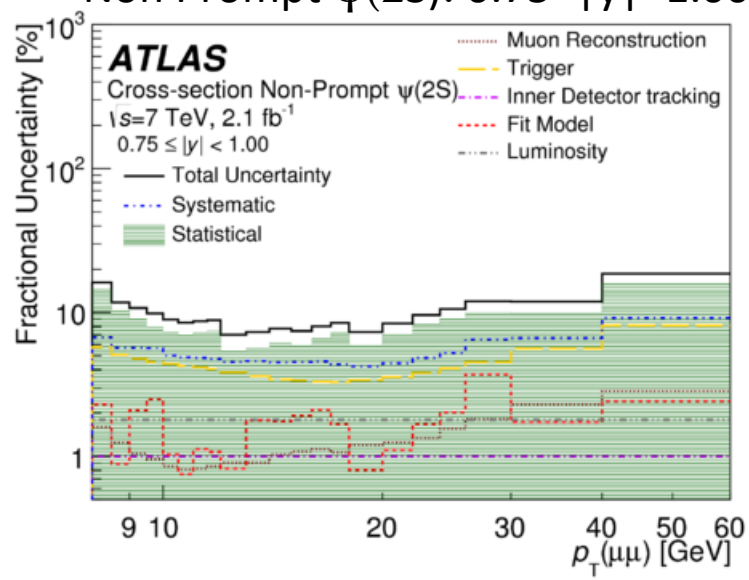

"Prompt" production compared with NLO-NRQCD:

→ fair agreement for the whole $P_T$ range for both J/ψ and ψ(2S)

→ no observed dependence on rapidity in theory/data ratio

**ψ(2S): √s=8 TeV**

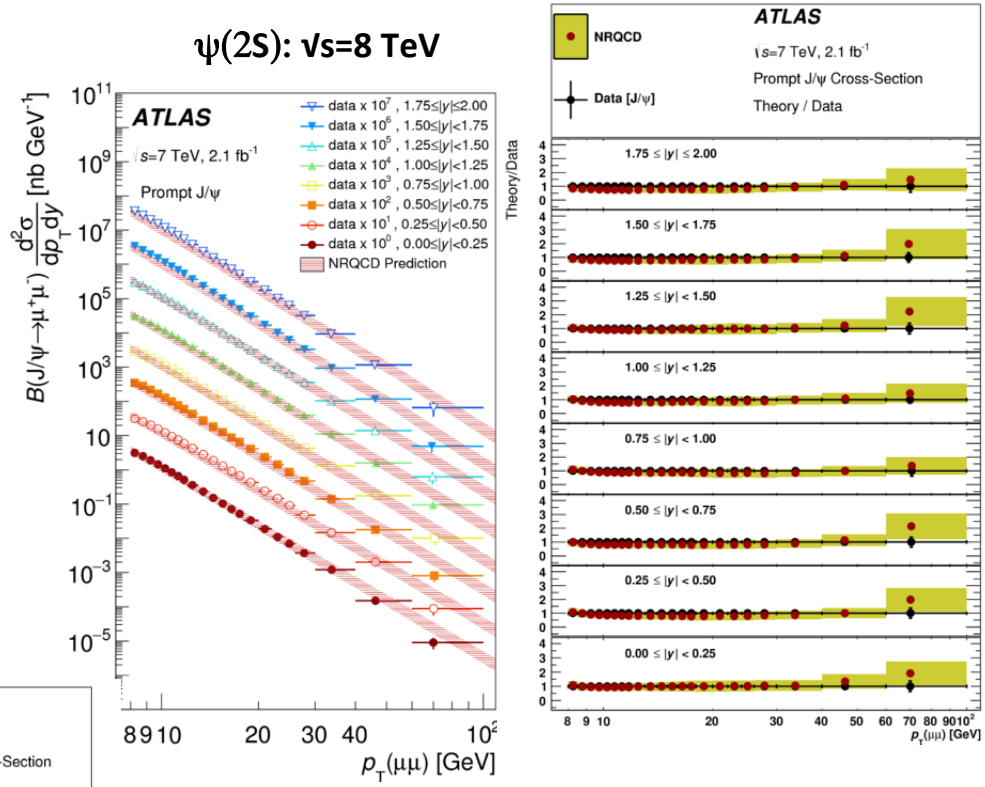


**J/ψ: √s=7 TeV**

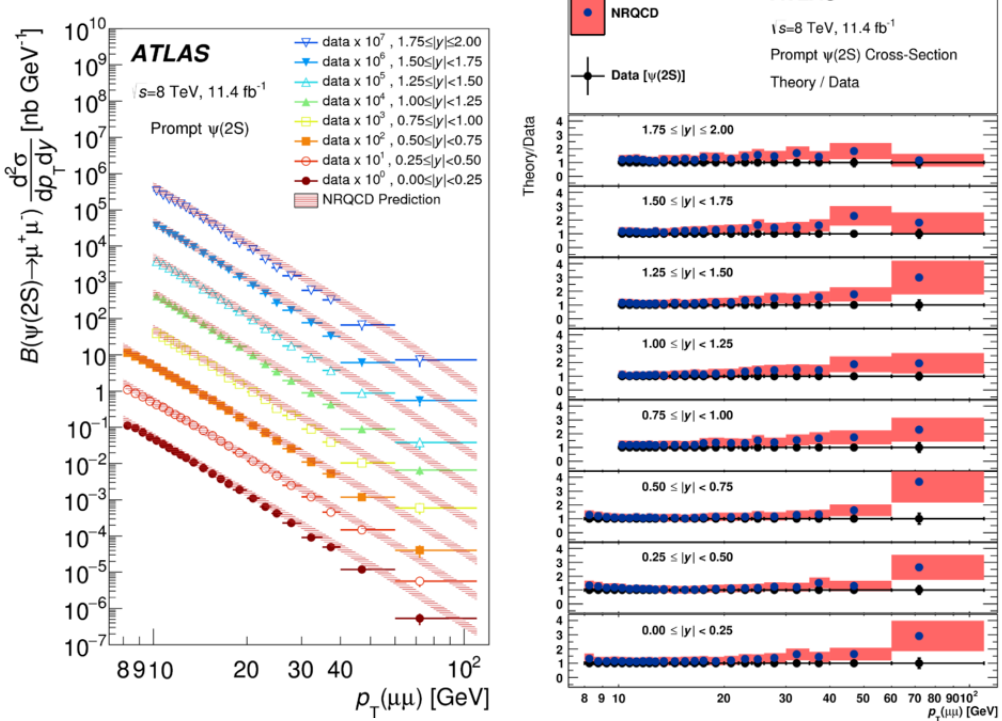

"NON-Prompt" production compared with FONLL for b-production followed b→ "ψ"+X

→ for J/ψ theory predicts "harder" spectra, for ψ(2S) theory predicts "higher" yield

→ no observed dependence on rapidity in theory/data ratio

**ψ(2S): √s=7 TeV**

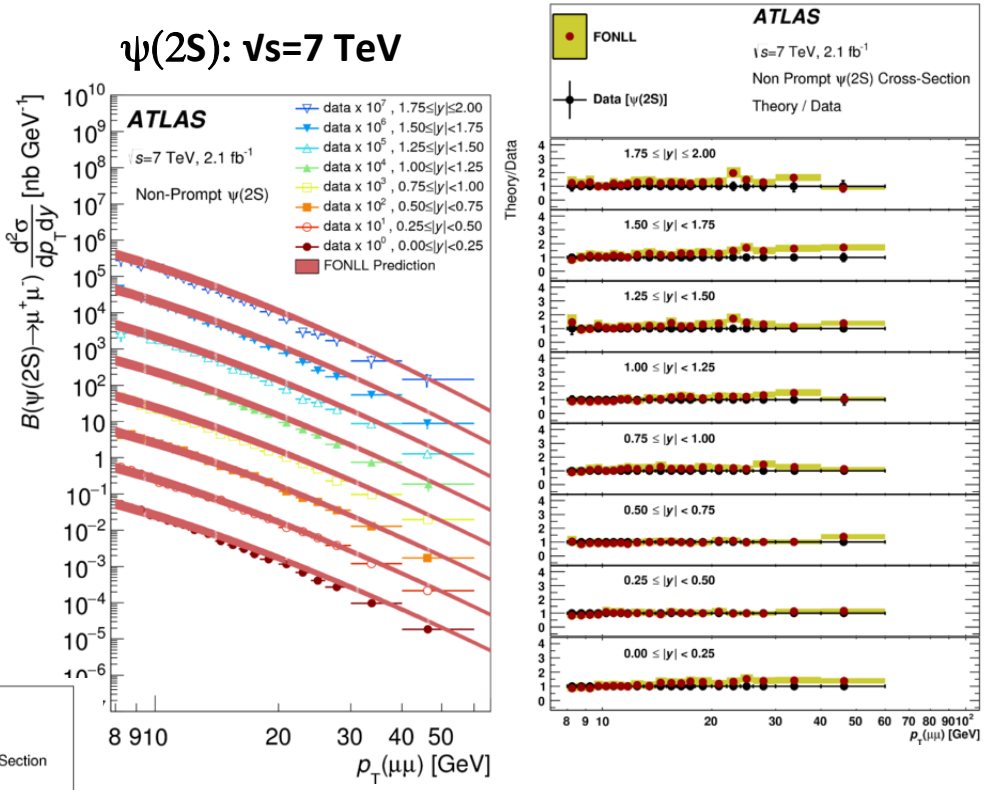


**J/ψ: √s=8 TeV**

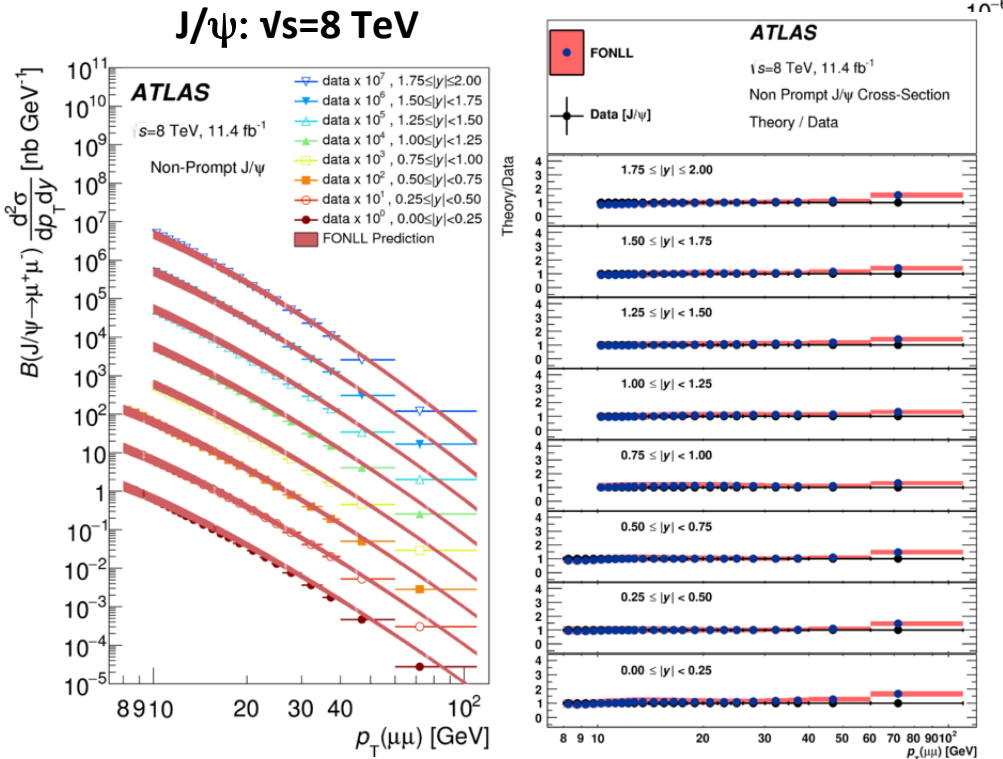


with the ATLAS experiment at LHC- LHCP 2016

# Non-prompt fraction of ψ

$$\mathbf{f_b^{\psi} \equiv \frac{pp \to b + X \to \psi + X'}{pp \xrightarrow{inclusive} \psi + x'} = \frac{N_{\psi}^{np}}{N_{\psi}^{np} + N_{\psi}^{p}}}$$

→ in each y-slice $f_b^{\psi}$ increases as function of $p_T$ without strong dependence on either y or √s

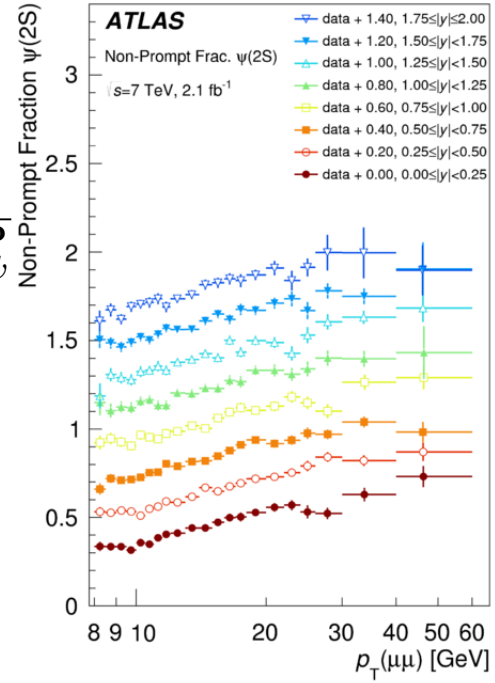


ψ(2S): √s=7 TeV

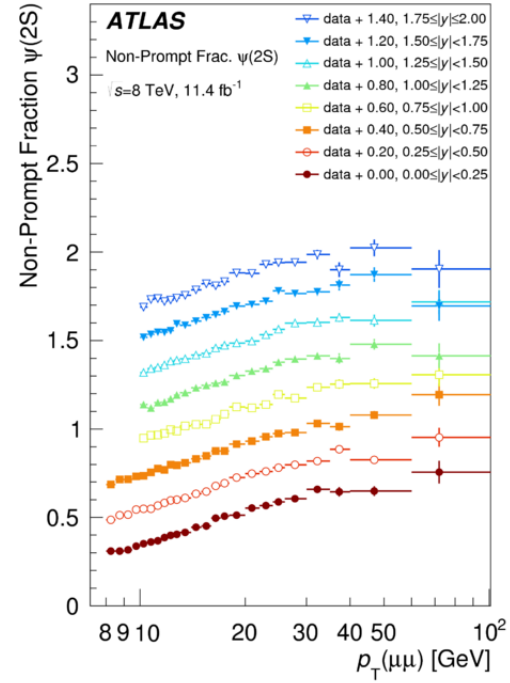


ψ(2S): √s=8 TeV

J/ψ: √s=7 TeV

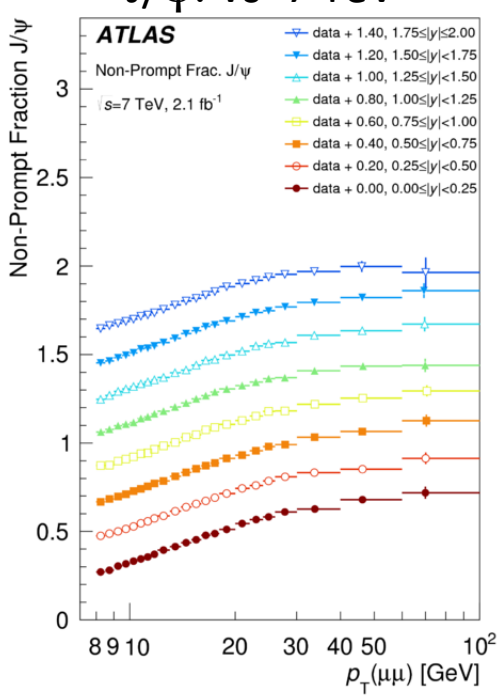


J/ψ: √s=8 TeV

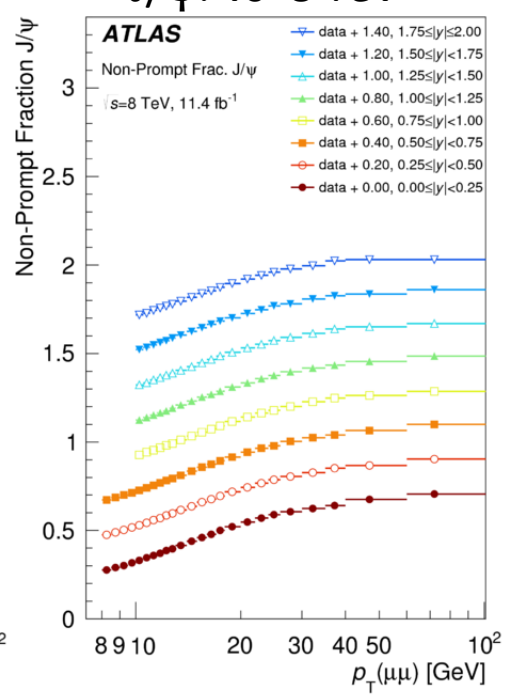

# Ratio of ψ(2S) to J/ψ for prompt and non-prompt

$$R^p = \frac{N^p_{\psi(2s)}}{N^p_{J/\psi}} \text{ and } R^{np} = \frac{N^{np}_{\psi(2s)}}{N^{np}_{J/\psi}}$$

→ $R^p$ slightly increase with $p_T$ while $R^{np}$ is flat, both without strong dependence on either y or √s

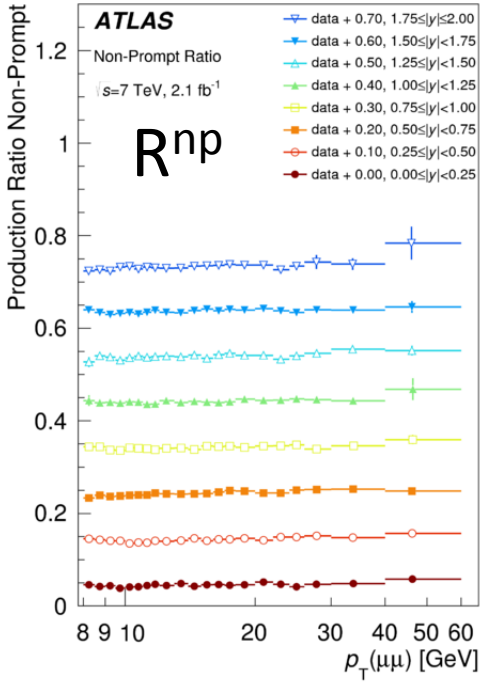


$R^{np}$: √s=7 TeV

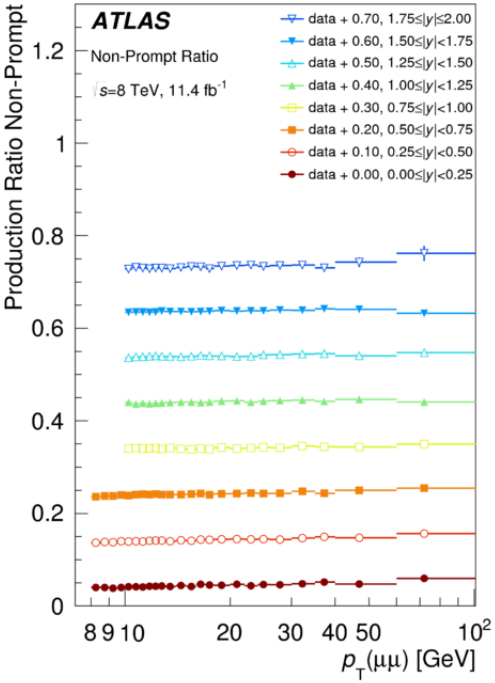


$R^{np}$: √s=8 TeV

$R^p$: √s=7 TeV

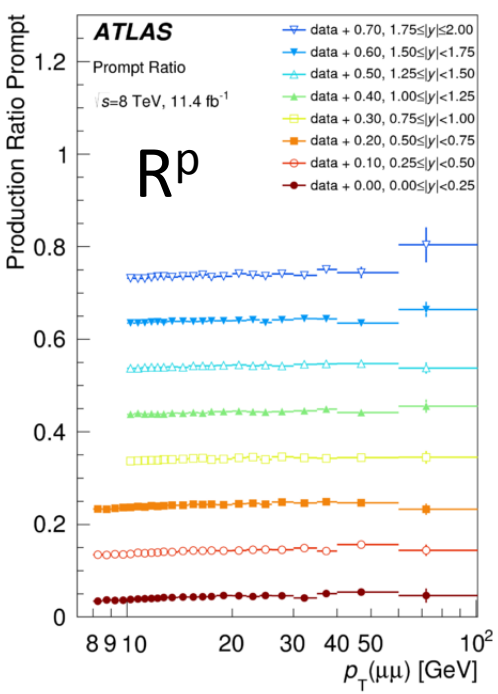


$R^p$: √s=8 TeV

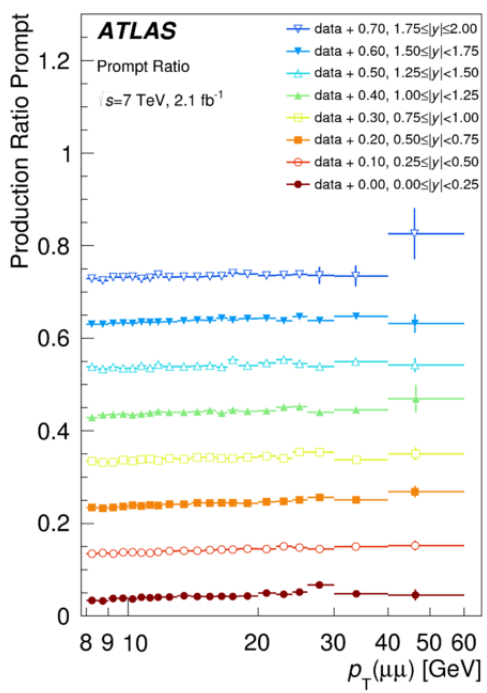

# B.2 J/ψ differential non prompt production at √s =13 TeV ATLAS-CONF-2015-030

$$f_b^{J/\psi} = \frac{N_{J/\psi}^{np}}{N_{J/\psi}^{np} + N_{J/\psi}^{p}}$$

Non-prompt fraction for J/ψ:
→ 6.4 pb$^{-1}$ at or √s=13 TeV
→ "first" simplified analysis due to large cancellations of uncertainties in the ratio
→ 3 y-bins 0.00-0.75-1.50-2.00

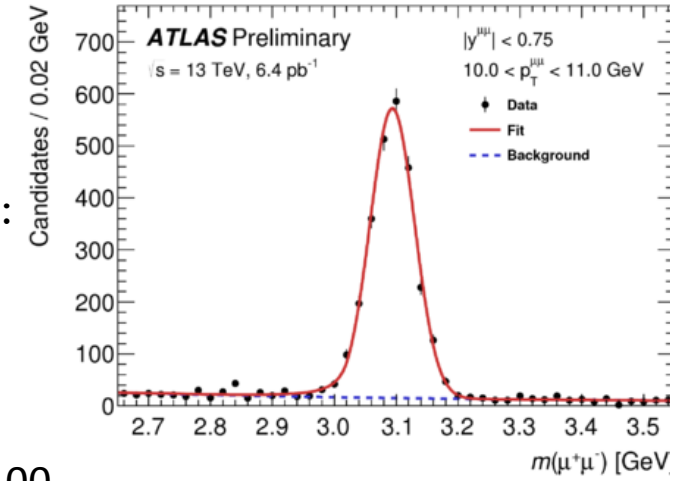


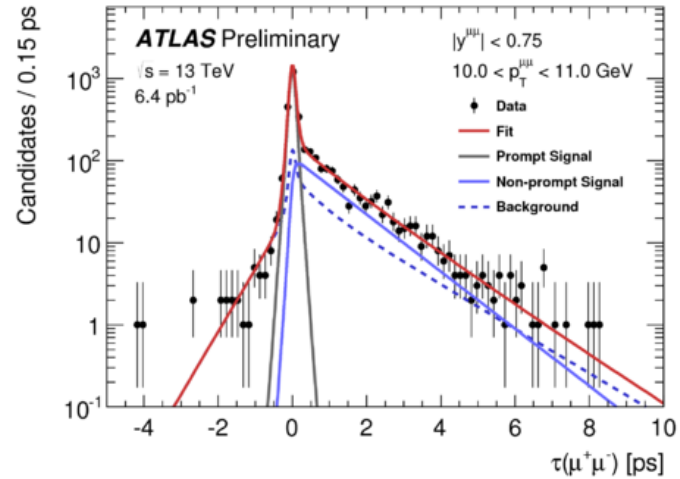

# B.2 J/ψ differential non prompt production at √s =13 TeV ATLAS-CONF-2015-030

$$f_b^{J/\psi} = \frac{N^{np}_{J/\psi}}{N^{np}_{J/\psi} + N^{p}_{J/\psi}}$$

Non-prompt fraction for J/ψ:
→ 6.4 pb$^{-1}$ at or √s=13 TeV
→ "first" simplified analysis due to large cancellations of uncertainties in the ratio
→ 3 y-bins 0.00-0.75-1.50-2.00

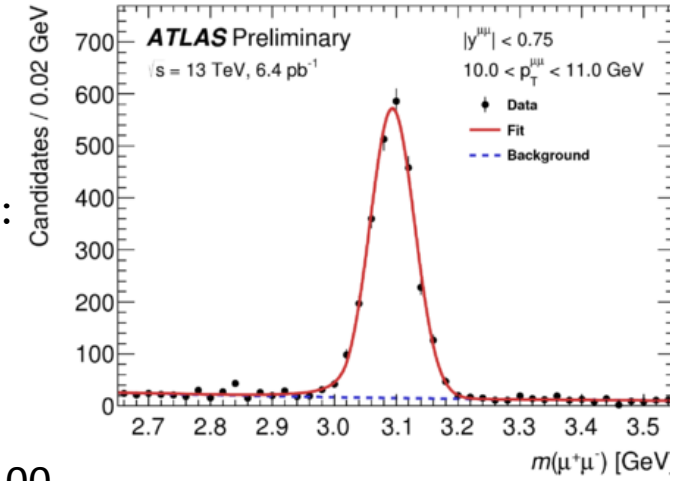


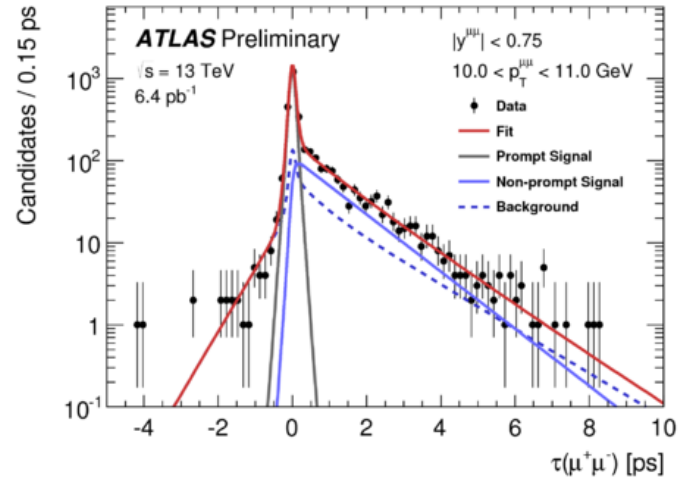


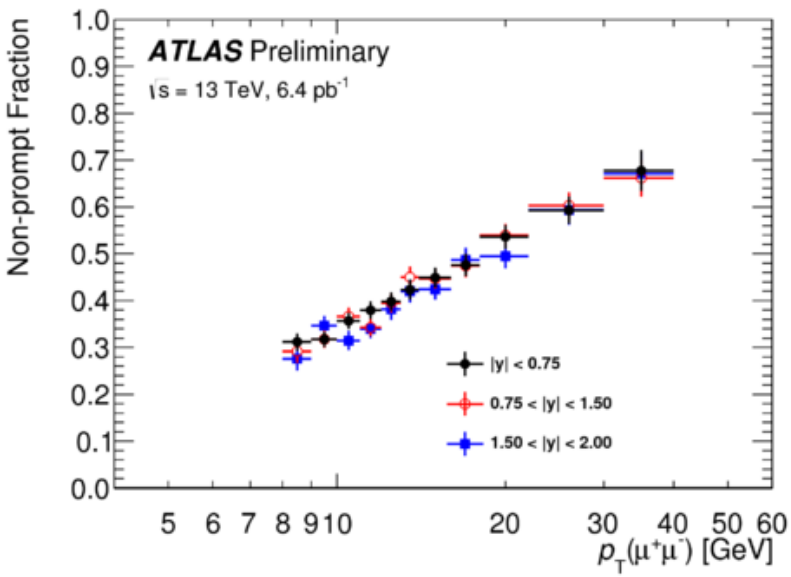


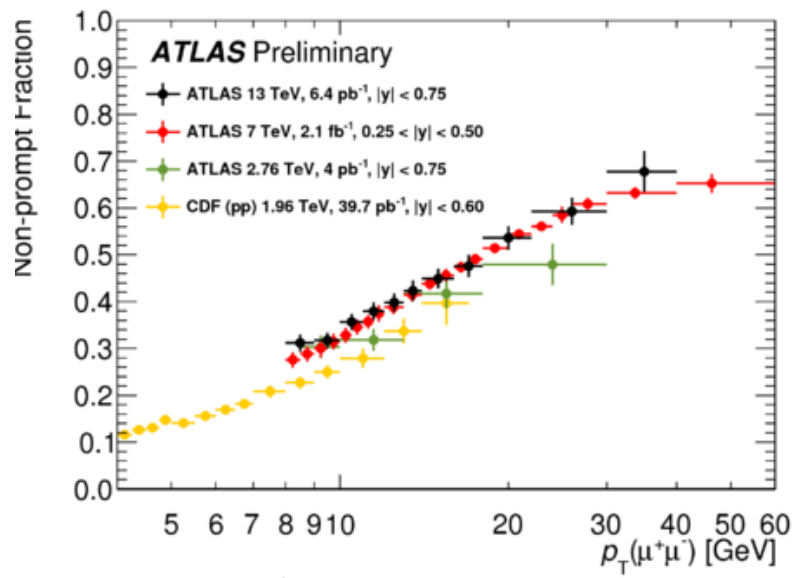


→ significant dependence on $p_T$ (0.25 at 8 Gev → 0.65 at 40 GeV) and no dependence on y
→ no significant change between √s=7 TeV and √s=13 TeV, contrary to significant difference between √s=7 TeV and lower energies (ATLAS √s=2.76 TeV AND CDF √s=1.96 TeV)

# C.1 $f_s/f_d$ determination at $\sqrt{s}$ =7 TeV

Phys. Rev. Lett. 115, 262001 (2015)

b-fragmentation fractions : $f_i = \mathcal{P}rob[\bar{b} \to (\bar{b}q_i)]$

$$q_i \equiv u, d, s, c \Rightarrow f_u + f_d + f_s + f_c + f_{baryon} = 1$$

→ important measurement for rare decays, searches, cross sections

$$\mathcal{L} = 2.47\, fb^{-1} \text{ at } \sqrt{s} = 7\,\text{TeV} \Rightarrow \begin{cases} B_s^0 \to J/\psi(\mu^+\mu^-)\ \phi(K^+K^-) \\ B_d^0 \to J/\psi(\mu^+\mu^-)\ K^{*0}(K^+\pi^-) \end{cases}$$

$$\frac{f_s}{f_d} = \frac{N_{B_s^0}}{N_{B_d^0}} \frac{\mathcal{B}\left(B_d^0 \to J/\psi\, K^{*0}\right)}{\mathcal{B}\left(B_s^0 \to J/\psi\, \phi\right)} \frac{\mathcal{B}\left(K^{*0} \to K^-\pi^+\right)}{\mathcal{B}\left(\phi \to K^+K^-\right)} \mathcal{R}_{eff}$$

$\mathcal{R}_{eff}$ relative efficiencies (acceptance and selection) from MC sample

$\mathcal{B}$ branching fractions of the relevant decay modes (world averages)

# C.1 $f_s/f_d$ determination at $\sqrt{s}$ =7 TeV

Phys. Rev. Lett. 115, 262001 (2015)

b-fragmentation fractions : $f_i = \mathcal{P}rob[\bar{b} \to (\bar{b}q_i)]$

$$q_i \equiv u, d, s, c \Rightarrow f_u + f_d + f_s + f_c + f_{baryon} = 1$$

→ important measurement for rare decays, searches, cross sections

$$\mathcal{L} = 2.47\, fb^{-1} \text{ at } \sqrt{s} = 7\,\text{TeV} \Rightarrow \begin{cases} B_s^0 \to J/\psi(\mu^+\mu^-)\ \phi(K^+K^-) \\ B_d^0 \to J/\psi(\mu^+\mu^-)\ K^{*0}(K^+\pi^-) \end{cases}$$

$$\frac{f_s}{f_d} = \frac{N_{B_s^0}}{N_{B_d^0}} \frac{\mathcal{B}\left(B_d^0 \to J/\psi\, K^{*0}\right)}{\mathcal{B}\left(B_s^0 \to J/\psi\, \phi\right)} \frac{\mathcal{B}\left(K^{*0} \to K^-\pi^+\right)}{\mathcal{B}\left(\phi \to K^+K^-\right)} \mathcal{R}_{eff}$$

$\mathcal{R}_{eff}$ relative efficiencies (acceptance and selection) from MC sample

$\mathcal{B}$ branching fractions of the relevant decay modes (world averages)

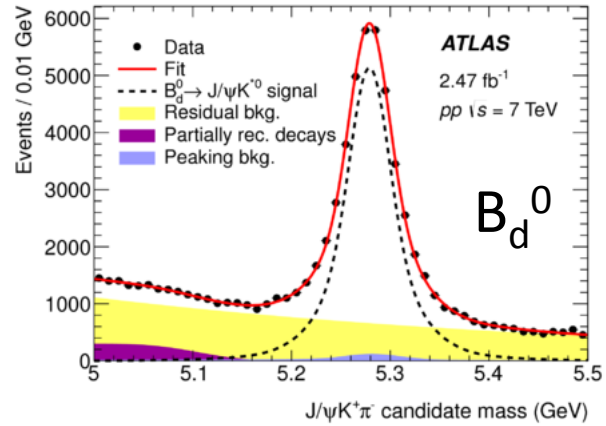


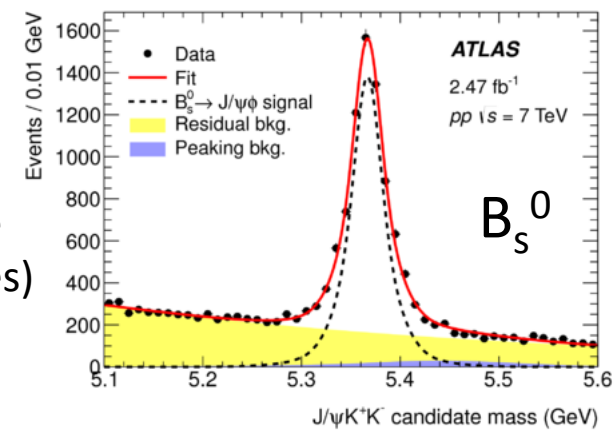


| Observable | Value | $\sigma$ |
|---|---|---|
| $N_{B_s^0}$ | $6640 \pm 100 \pm 220$ | 3.3% |
| $N_{B_d^0}$ | $36290 \pm 320 \pm 650$ | 1.8% |
| $\mathcal{R}_{\text{eff}}$ | $0.799 \pm 0.001 \pm 0.010$ | 1.3% |
| $\mathcal{B}(\phi \to K^+K^-)$ | $0.489 \pm 0.005$ | 1.0% |
| $\mathcal{B}(K^{*0} \to K^+\pi^-)$ | $0.66503 \pm 0.00014$ | 0.02% |
| Total | | 4.1% |

$$\frac{f_s}{f_d} \cdot \frac{\mathcal{B}\left(B_s^0 \to J/\psi\, \phi\right)}{\mathcal{B}\left(B_d^0 \to J/\psi\, K^{*0}\right)} = 0.199 \begin{cases} \pm 0.004(\text{stat}) \\ \pm 0.008(\text{syst.}) \end{cases}$$

→ Ratio of $\mathcal{B}$s is better estimated from theory than from measurement, recent results (Phys. Rev. D89 (2014) 094010 and arXiv:1309.0313v2) has global 7.1% uncertainty:

$$\frac{\mathcal{B}\left(B_s^0 \to J/\psi\,\phi\right)}{\mathcal{B}\left(B_d^0 \to J/\psi\,K^{*0}\right)} = 0.83^{+0.03}_{-0.02}(\omega_B)^{+0.01}_{-0.00}(f_M)^{+0.01}_{-0.02}(a_i)^{+0.01}_{-0.02}(m_c)$$

$$\Rightarrow \frac{f_s}{f_d} = 0.240 \pm 0.004(\text{stat.}) \pm 0.010(\text{syst.}) \pm 0.017(\text{theo.})$$

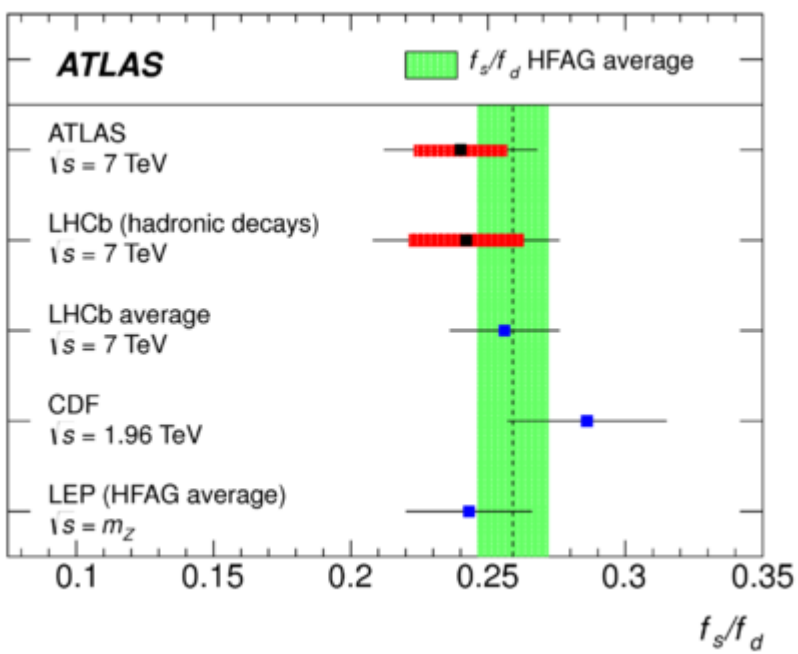


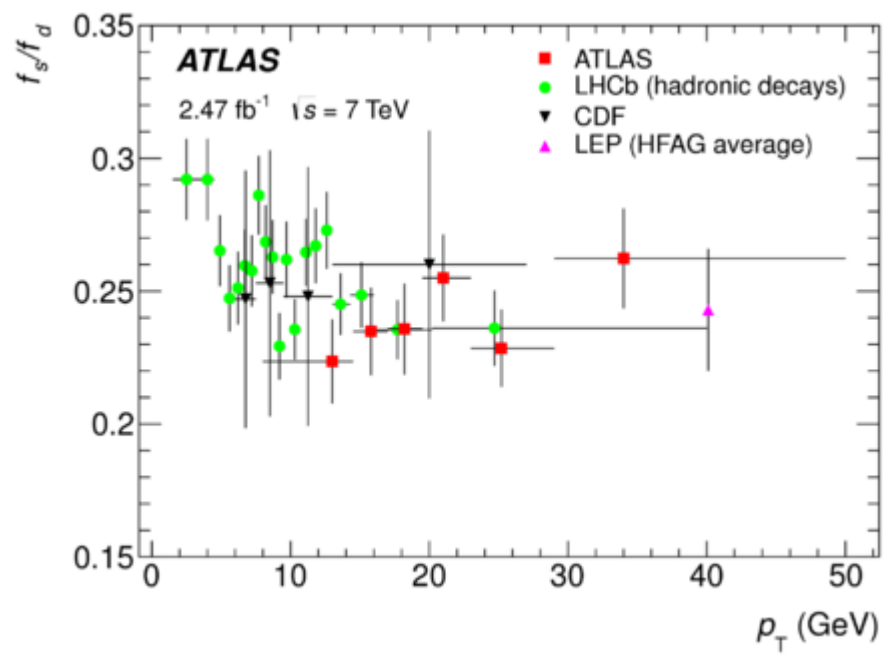


→ no significant dependence on $p_T$ or $\eta$

# C.2 $B^{\pm}$ mass reconstruction in $B^{\pm} \rightarrow J/\psi\ K^{\pm}$ at $\sqrt{s}$ =13 TeV ATLAS-CONF-2015-064

$$B^+ \rightarrow J/\psi(\mu^+\mu^-)\ + K^+,\ \mathcal{L} = 3.2\, fb^{-1} \text{ at } \sqrt{s} = 13\,\text{TeV}$$

$$|y| < 2.5,\ \text{dependence of mass resolution on y}$$

$$|y| < 1.75\,\text{bins of } \Delta y = 0,25\ + 1.75 < |y| < 2.50\,\text{bins}$$

Important test of ATLAS tracking capability for future B-physics

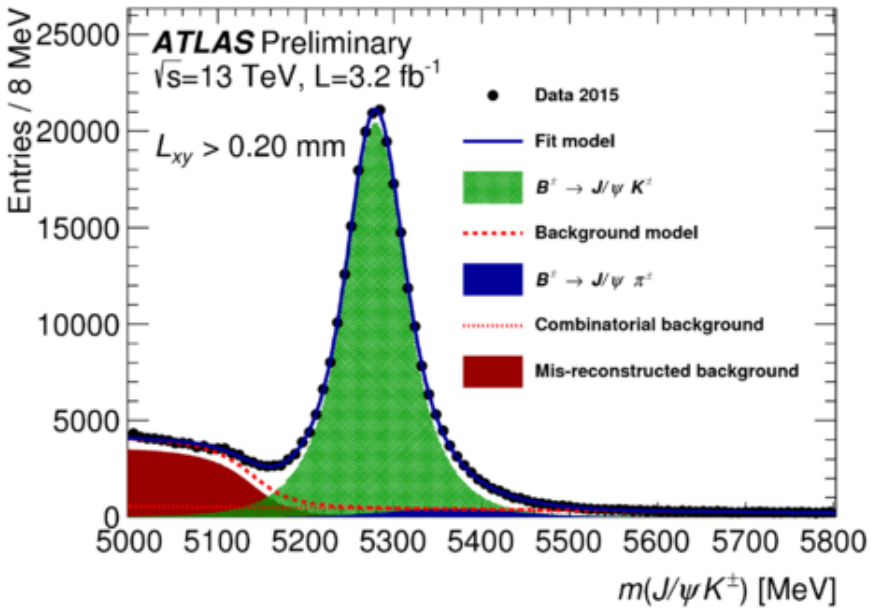


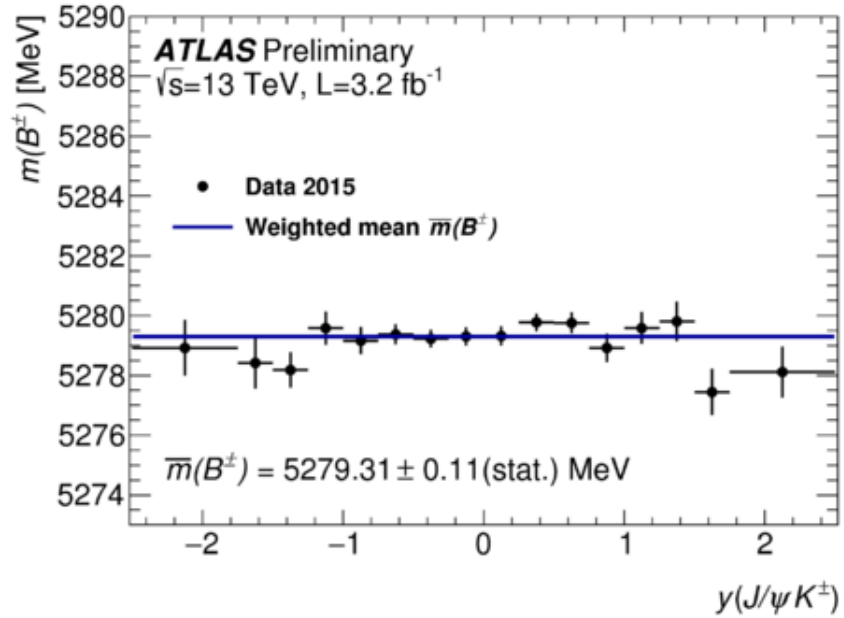

# C.2 $B^{\pm}$ mass reconstruction in $B^{\pm} \rightarrow J/\psi\ K^{\pm}$ at $\sqrt{s}$ =13 TeV ATLAS-CONF-2015-064

$$B^+ \rightarrow J/\psi(\mu^+\mu^-)\ + K^+,\ \mathcal{L} = 3.2\, fb^{-1} \text{ at } \sqrt{s} = 13\,\text{TeV}$$

$$|y| < 2.5,\ \text{dependence of mass resolution on y}$$

$$|y| < 1.75\,\text{bins of } \Delta y = 0,25\ + 1.75 < |y| < 2.50\,\text{bins}$$

Important test of ATLAS tracking capability for future B-physics

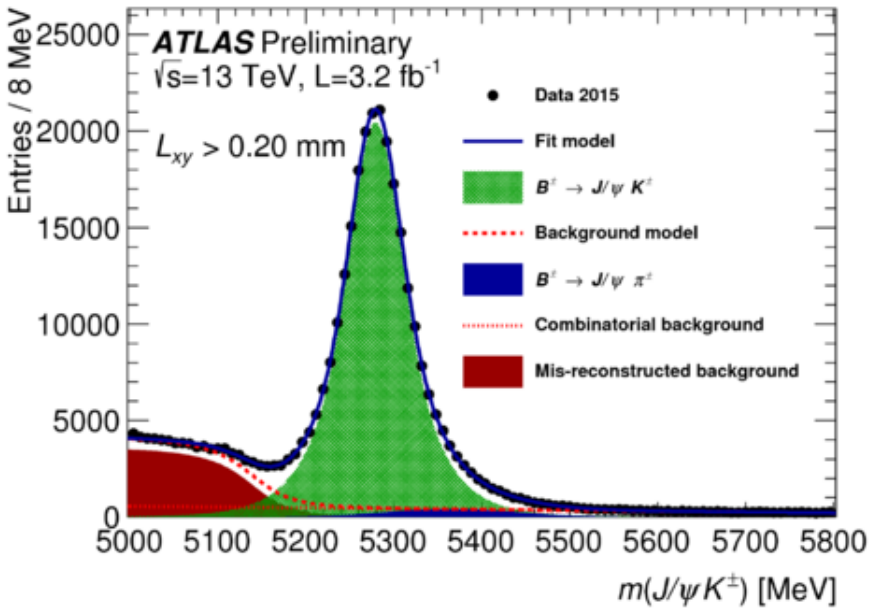


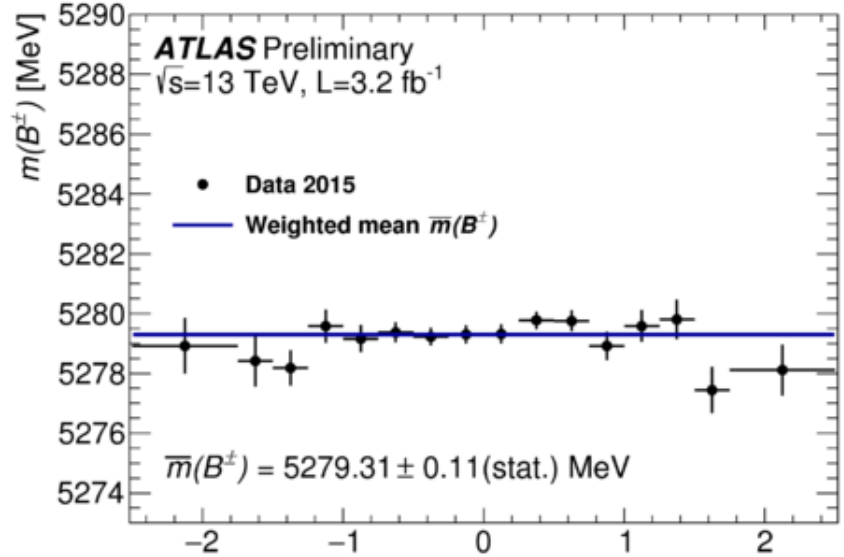


| Fit | $B^{\pm}$ mass [MeV] | Fit error [MeV] |
|---|---|---|
| Default Fit | 5279.31 | 0.11 (stat.) |
| $L_{xy}$ > 0.2 mm | 5279.34 | 0.09 (stat.) |
| World Average fit | 5279.29 | 0.15 |
| LHCb | 5279.38 | 0.11 (stat.) ± 0.33 (syst.) |

| Source | Systematic Error [MeV] |
|---|---|
| $y$-Dependence | 0.11 |
| Signal Mass Model | 0.09 |
| Background Mass Model | 0.17 |
| Mass Fit Window | 0.14 |
| $B^{\pm} \rightarrow J/\psi\pi^{\pm}$ Background: | |
| Fraction | 0.02 |
| Line Shape | 0.04 |
| MC Reweighting | 0.04 |
| Total | 0.25 |

good agreement with World Average → validation of momentum calibration of the ID of ATLAS

# C.3 $D^{*\pm}$ , $D^{\pm}$ and $D_s^{\pm}$ production at $\sqrt{s}$ =7 TeV

Nucl.Phys. B907 (2016) 717

2010 data taking at $\sqrt{s}$=7 TeV → fiducial phase space region $3.5<p_T^{(D)}<100$ GeV and $|\eta^{(D)}|<2.1$

$$\text{two trigger data sample} \begin{cases} \text{low}\, p_T \in [3.5,\ 20]\text{GeV} \Rightarrow\ Minimum\ bias/Random \rightarrow \mathcal{L} = 1.04\, nb^{-1} \\ \text{high}\, p_T \in [20, 100]\text{GeV} \Rightarrow\ Jet\ Trigger\ E \geq 15\,\text{GeV} \rightarrow\ \mathcal{L} = 280\, nb^{-1} \end{cases}$$

# C.3 $D^{*\pm}$, $D^{\pm}$ and $D_s^{\pm}$ production at $\sqrt{s}$ =7 TeV

Nucl.Phys. B907 (2016) 717

2010 data taking at $\sqrt{s}$=7 TeV → fiducial phase space region $3.5<p_T^{(D)}<100$ GeV and $|\eta^{(D)}|<2.1$

two trigger data sample

$$\begin{cases} \text{low } p_T \in [3.5,\ 20]\text{GeV} \Rightarrow\ Minimum\ bias/Random \rightarrow \mathcal{L} = 1.04\, nb^{-1} \\ \text{high } p_T \in [20, 100]\text{GeV} \Rightarrow\ Jet\ Trigger\ E \geq 15\,\text{GeV} \rightarrow\ \mathcal{L} = 280\, nb^{-1} \end{cases}$$

$D^{*+} \rightarrow D^0\ \pi_s$ $\quad D^0 \rightarrow K^-\pi^+$ $\qquad D^+ \rightarrow K^-\pi^+\pi^+$ $\qquad D_s^+ \rightarrow \phi\ \pi^+$ $\quad \phi \rightarrow K^+K^-$

"low " $p_T$

"high " $p_T$

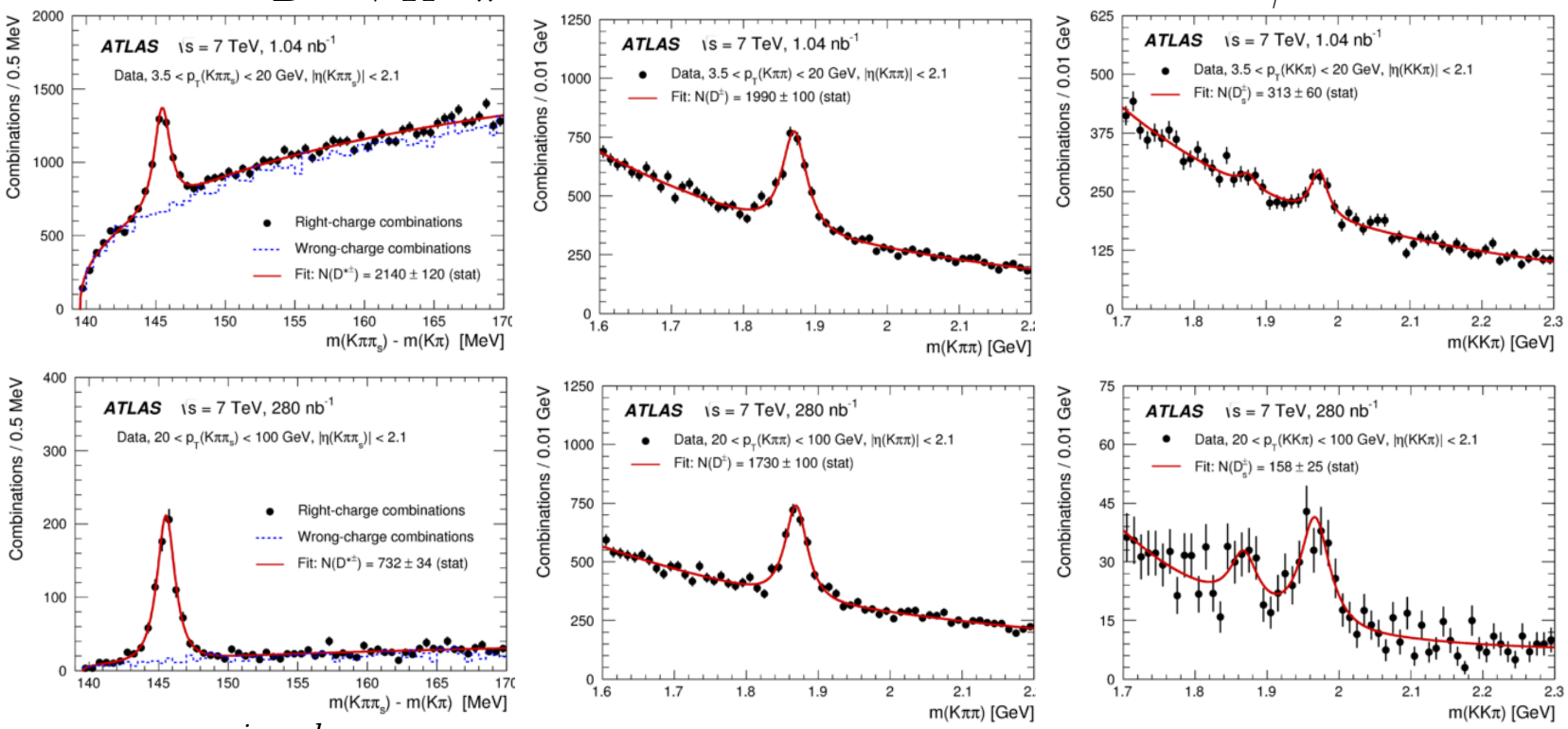


$$Fit: \quad \overbrace{\text{Gauss}^{mod} \propto e^{-\frac{1}{2}x^{1+\frac{1}{1+0.5x}}}}^{signal} + \overbrace{\text{threshold function or quadratic exponential}}^{background}$$

Visible cross sections in "low" and "high" $p_T$ regions:

$$\sigma_{pp\to D\,X} = \frac{N(D)}{\mathcal{A}\cdot\mathcal{L}\cdot\mathcal{B}}$$

- $\mathcal{A}$ from MC sample
- $\mathcal{B}$ world average

Systematic uncertainties dominated :

- Tracking (detector material in MC);
- Luminosity and $\mathcal{B}$ for $D_s$

| Source | $\sigma^{\rm vis}(D^{*\pm})$ | | $\sigma^{\rm vis}(D^{\pm})$ | | $\sigma^{\rm vis}(D_s^{\pm})$ | |
|---|---|---|---|---|---|---|
| | Low-$p_T$ | High-$p_T$ | Low-$p_T$ | High-$p_T$ | Low-$p_T$ | High-$p_T$ |
| Trigger ($\delta_1$) | - | $^{+0.9}_{-1.0}\%$ | | $^{+0.9}_{-1.0}\%$ | - | $^{+0.9}_{-1.0}\%$ |
| Tracking ($\delta_2$) | ±7.8% | ±7.4% | ±7.7% | ±7.4% | ±7.6% | ±7.4% |
| $D$ selection ($\delta_3$) | $^{+2.8}_{-1.6}\%$ | $^{+1.7}_{-1.4}\%$ | $^{+1.6}_{-1.0}\%$ | $^{+0.9}_{-0.6}\%$ | $^{+2.6}_{-1.6}\%$ | $^{+1.1}_{-0.9}\%$ |
| Signal fit ($\delta_4$) | ±1.3% | ±0.9% | ±1.3% | ±1.5% | ±6.4% | ±5.3% |
| Modelling ($\delta_5$) | $^{+1.0}_{-1.7}\%$ | $^{+2.7}_{-2.3}\%$ | $^{+2.3}_{-2.6}\%$ | $^{+2.9}_{-2.4}\%$ | $^{+1.7}_{-2.4}\%$ | $^{+2.8}_{-2.4}\%$ |
| Size of MC sample ($\delta_6$) | ±0.6% | ±0.9% | ±0.8% | ±0.8% | ±2.9% | ±3.1% |
| Luminosity ($\delta_7$) | ±3.5% | ±3.5% | ±3.5% | ±3.5% | ±3.5% | ±3.5% |
| Branching fraction ($\delta_8$) | ±1.5% | ±1.5% | ±2.1% | ±2.1% | ±5.9% | ±5.9% |

Visible cross sections in "low" and "high" $p_T$ regions:

$$\sigma_{pp\to D\,X} = \frac{N(D)}{\mathcal{A}\cdot\mathcal{L}\cdot\mathcal{B}}$$

- $\mathcal{A}$ from MC sample
- $\mathcal{B}$ world average

Systematic uncertainties dominated :

- Tracking (detector material in MC);
- Luminosity and $\mathcal{B}$ for $D_s$

| Source | $\sigma^{vis}(D^{*\pm})$ | | $\sigma^{vis}(D^{\pm})$ | | $\sigma^{vis}(D_s^{\pm})$ | |
|---|---|---|---|---|---|---|
| | Low-$p_T$ | High-$p_T$ | Low-$p_T$ | High-$p_T$ | Low-$p_T$ | High-$p_T$ |
| Trigger ($\delta_1$) | - | $^{+0.9}_{-1.0}$% | | $^{+0.9}_{-1.0}$% | - | $^{+0.9}_{-1.0}$% |
| Tracking ($\delta_2$) | ±7.8% | ±7.4% | ±7.7% | ±7.4% | ±7.6% | ±7.4% |
| $D$ selection ($\delta_3$) | $^{+2.8}_{-1.6}$% | $^{+1.7}_{-1.4}$% | $^{+1.6}_{-1.0}$% | $^{+0.9}_{-0.6}$% | $^{+2.6}_{-1.6}$% | $^{+1.1}_{-0.9}$% |
| Signal fit ($\delta_4$) | ±1.3% | ±0.9% | ±1.3% | ±1.5% | ±6.4% | ±5.3% |
| Modelling ($\delta_5$) | $^{+1.0}_{-1.7}$% | $^{+2.7}_{-2.3}$% | $^{+2.3}_{-2.6}$% | $^{+2.9}_{-2.4}$% | $^{+1.7}_{-2.4}$% | $^{+2.8}_{-2.4}$% |
| Size of MC sample ($\delta_6$) | ±0.6% | ±0.9% | ±0.8% | ±0.8% | ±2.9% | ±3.1% |
| Luminosity ($\delta_7$) | ±3.5% | ±3.5% | ±3.5% | ±3.5% | ±3.5% | ±3.5% |
| Branching fraction ($\delta_8$) | ±1.5% | ±1.5% | ±2.1% | ±2.1% | ±5.9% | ±5.9% |

| | $\sigma^{vis}(D^{*\pm})$ | | $\sigma^{vis}(D^{\pm})$ | | $\sigma^{vis}(D_s^{*\pm})$ | |
|---|---|---|---|---|---|---|
| Range [units] | low-$p_T$ [μb] | high-$p_T$ [nb] | low-$p_T$ [μb] | high-$p_T$ [nb] | low-$p_T$ [μb] | high-$p_T$ [nb] |
| ATLAS | 331 ± 36 | 988 ± 100 | 328 ± 34 | 888 ± 97 | 160 ± 37 | 512 ± 104 |
| GM-VFNS | $340^{+130}_{-150}$ | $1000^{+120}_{-150}$ | $350^{+150}_{-160}$ | $980^{+120}_{-150}$ | $147^{+54}_{-66}$ | $470^{+56}_{-69}$ |
| FONLL | $202^{+125}_{-79}$ | $753^{+123}_{-104}$ | $174^{+105}_{-66}$ | $617^{+103}_{-86}$ | - | - |
| POWHEG+PYTHIA | $158^{+179}_{-85}$ | $600^{+300}_{-180}$ | $134^{+148}_{-70}$ | $480^{+240}_{-130}$ | $62^{+64}_{-31}$ | $225^{+114}_{-69}$ |
| POWHEG+HERWIG | $137^{+147}_{-72}$ | $690^{+380}_{-160}$ | $121^{+129}_{-64}$ | $580^{+280}_{-140}$ | $51^{+50}_{-25}$ | $268^{+107}_{-62}$ |
| MC@NLO | $157^{+125}_{-72}$ | $980^{+460}_{-290}$ | $140^{+112}_{-65}$ | $810^{+390}_{-260}$ | $58^{+42}_{-25}$ | $345^{+175}_{-87}$ |

Comparison of visible cross sections with predictions:
→agreement with GM-VFNS;
→ for FONLL, POWHEG, MC@NLO the central values are lower than data but are consistent including theoretical uncertainties due to: μ scales, $m_Q$, PDFs, $f_{Q\to D}$

Extrapolation from "visible" → total phase space → total charm cross sections with FONLL for low $p_T$ sample and only for $D^{*+}$ and $D^+$

$$\sigma_{c\bar{c}}^{tot} = 8.6 \pm 0.3(\text{stat.}) \pm 0.7(\text{syst.}) \pm 0.3(\text{lum.}) \pm 0.2(\text{ff.})^{+3.8}_{-3.4}(\text{extr.})\,\text{mb}\ (\text{ATLAS})$$

$$\sigma_{c\bar{c}}^{tot} = 8.5 \pm 0.5(\text{stat.})\,^{+1.0}_{-2.4}(\text{syst.}) \pm 0.3(\text{lum.}) \pm 0.2(\text{ff.})^{+5.0}_{-0.4}(\text{extra.})\,\text{mb}\ (\text{ALICE})$$

# Differential cross section in $p_T$ and $\eta$ for $D^{*+}$ and $D^+$

Comparison of data with theoretical predictions:

- in general theory below data but consistent within uncertainties;
- the shape of $p_T$ spectra well reproduced by FONLL, POWHEG while MC@NLO slightly harder;
- $\eta$ shape for high $p_T$ of MC@NLO prediction differs from the data;
- GM-VFSN predictions agree both in shape and normalization

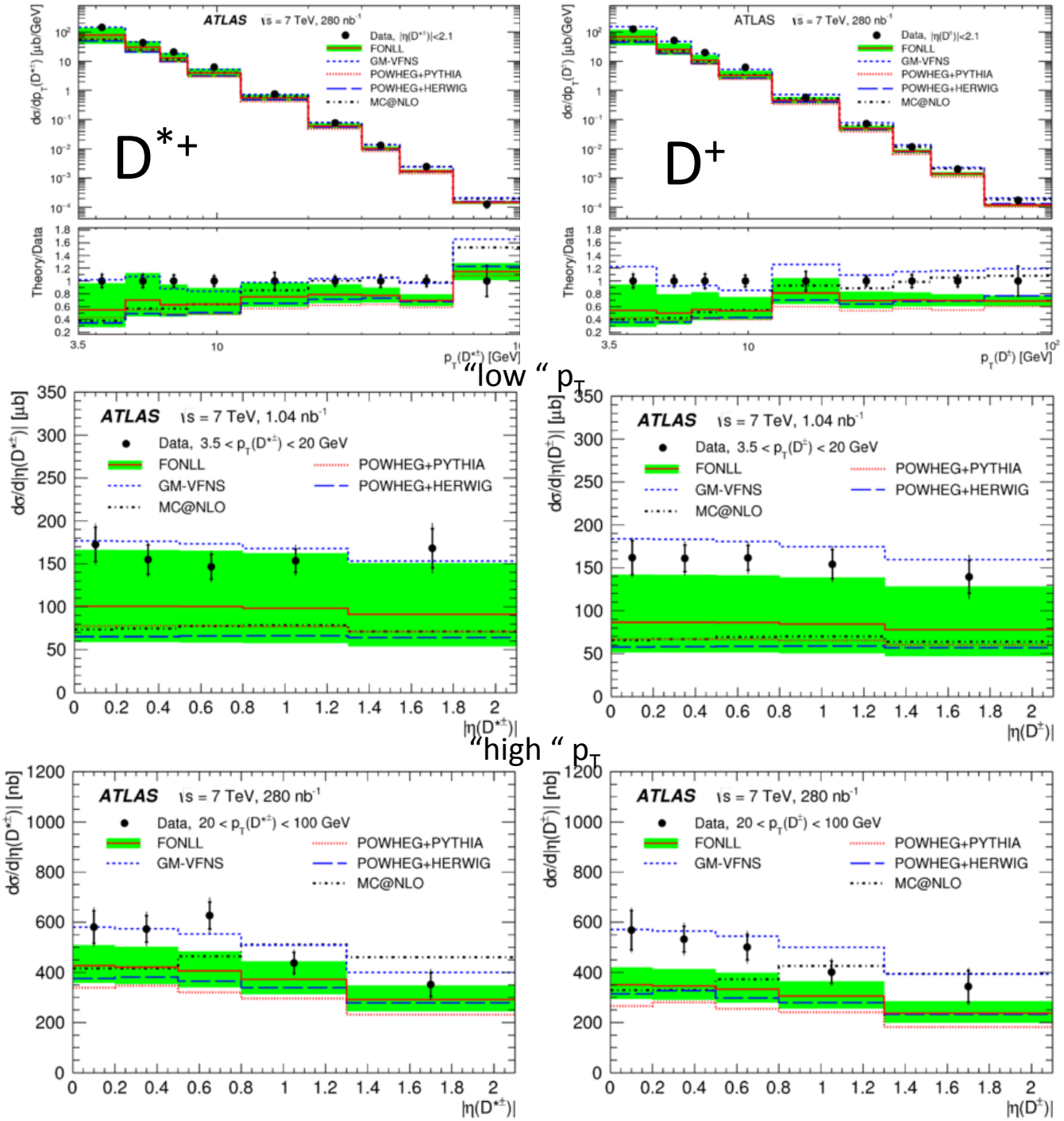

# Conclusions

- LHC performances allowed ATLAS to make high precision measurements in the production of quarkonium ($J/\psi$, $\psi_{2s}$,) and HF open state (b, $D^+$).
- At LHC new kinematical regions (e.g. high $p_T$) are available to deeply test the predictions of the different models for QCD.
- Expect to fully exploite run-II to confirm and probe new interesting phenomena in HF production even in challenging data-taking conditions for HF physics